PCCP

Cite this: *Phys. Chem. Chem. Phys.*, 2011, **13**, 15936–15946

www.rsc.org/pccp

PAPER

UV absorption cross sections between 230 and 350 nm and pressure dependence of the photolysis quantum yield at 308 nm of CF_3CH_2CHO†

María Antiñolo, Elena Jiménez and José Albaladejo*

Received 29th April 2011, Accepted 5th July 2011
DOI: 10.1039/c1cp21368g

Ultraviolet (UV) absorption cross sections of CF_3CH_2CHO were determined between 230 and 350 nm by gas-phase UV spectroscopy. The forbidden n → π* transition was characterized as a function of temperature (269–323 K). In addition, the photochemical degradation of CF_3CH_2CHO was investigated at 308 nm. The possible photolysis channels are: CF_3CH_2 + HCO (R1a), CF_3CH_3 + CO (R1b), and CF_3CH_2CO + H (R1c). Photolysis quantum yields of CF_3CH_2CHO at 308 nm, $\Phi_{\lambda=308\text{nm}}$, were measured as a function of pressure (25–760 Torr of synthetic air). The pressure dependence of $\Phi_{\lambda=308\text{nm}}$ can be expressed as the following Stern–Volmer equation: $1/\Phi_{\lambda=308\text{nm}} = (4.65 \pm 0.56) + (1.51 \pm 0.04) \times 10^{-18}$ [M] ([M] in molecule cm^{-3}). Using the absorption cross sections and the photolysis quantum yields reported here, the photolysis rate coefficient of this fluorinated aldehyde throughout the troposphere was estimated. This calculation shows that tropospheric photolysis of CF_3CH_2CHO is competitive with the removal initiated by OH radicals at low altitudes, but it can be the major degradation route at higher altitudes. Photodegradation products (CO, HC(O)OH, CF_3CHO, CF_3CH_2OH, and F_2CO) were identified and also quantified by Fourier transform infrared spectroscopy. $CF_3CH_2C(O)OH$ was identified as an end-product as a result of the chemistry involving CF_3CH_2CO radicals formed in the OH + CF_3CH_2CHO reaction. In the presence of an OH-scavenger (cyclohexane), $CF_3CH_2C(O)OH$ was not detected, indicating that channel (R1c) is negligible. Based on a proposed mechanism, our results provide strong evidences of the significant participation of the radical-forming channel (R1a).

Introduction

Fluorinated alcohols are potentially good alternatives for CFC replacements due to their zero ozone depletion potential (ODP) and low global warming potentials (GWP).[1,2] Homogeneous oxidation initiated by hydroxyl (OH) radicals and their uptake by cloud water and rain are the main atmospheric fates of partially fluorinated alcohols.[2–7] The major oxidation products of $CF_3(CH_2)_xCH_2OH$ (x = 0 and 1) are the corresponding fluorinated aldehydes, $CF_3(CH_2)_xCHO$.[2–5] To determine the environmental impact of these potentially secondary pollutants in the troposphere, their atmospheric lifetimes are needed. Determining the atmospheric lifetimes of aldehydes requires obtaining the rate coefficients for all the removal processes. These processes primarily include the reaction with OH radicals and ultraviolet (UV) photolysis in the actinic region ($\lambda \geq 290$ nm).

Several groups have performed gas-phase reactivity studies on CF_3CHO,[7] CF_3CH_2CHO,[3,4,8,9] and $CF_3CH_2CH_2CHO$[8] at room temperature. Recently, we reported the temperature dependence of the OH and Cl-rate coefficients for the reaction with CF_3CH_2CHO and $CF_3CH_2CH_2CHO$ in the 263–371 K range.[8] Lifetime due to homogeneous reactions for CF_3CH_2CHO is 4 days at the surface and 6 days at 10 km. At high altitudes, the solar actinic flux is higher than at the surface and the lifetime due to photolysis decreases with altitude. Therefore, UV photolysis in the actinic region is expected to be a significant sink of fluoroaldehydes in the troposphere. An evaluation of the photolysis rate throughout the troposphere, J, of CF_3CH_2CHO must be carried out in order to account for this degradation route. The photolysis rate of CF_3CH_2CHO in the actinic region is defined as:

$$J = \int_{\lambda > 290\,\text{nm}} \sigma_\lambda \Phi_\lambda F_\lambda \, d\lambda \qquad \text{(E1)}$$

Therefore, the wavelength and/or pressure dependence of the UV absorption cross sections (σ_λ) and the photolysis quantum yields (Φ_λ) of these species together with the spectral actinic flux (F_λ) in the troposphere are needed.

UV absorption cross sections in the 200–400 nm range and photolysis quantum yields for CF_3CHO and CF_3CH_2CHO have been reported by Sellevåg *et al.*[9] and Chiappero *et al.*[10] Sellevåg *et al.*[9] measured the effective quantum yield

Departamento de Química Física, Facultad de Ciencias Químicas, Universidad de Castilla-La Mancha, Avda. Camilo José Cela, s/n, 13071 Ciudad Real, Spain. E-mail: Jose.Albaladejo@uclm.es
† Electronic supplementary information (ESI) available. See DOI: 10.1039/c1cp21368g

($\Phi_{\lambda \geq 290\text{nm}}$) for CF_3CHO and CF_3CH_2CHO under pseudo-natural conditions in the European simulation chamber EUPHORE. Chiappero *et al.*[10] measured the photolysis quantum yield at 254 nm and 308 nm at a total pressure of N_2 of 700 Torr. However, no pressure dependence of the photolysis quantum yield for CF_3CH_2CHO has been reported to date.

Since temperature and total pressure in the troposphere decrease with altitude, a detailed study on the temperature and pressure dependence of σ_λ and Φ_λ is needed to better quantify this route. Hence, the aim of this work is to report the photolysis quantum yield of CF_3CH_2CHO at 308 nm ($\Phi_{308\text{nm}}$) and at different total pressures (25–760 Torr of synthetic air):

$$CF_3CH_2CHO + h\nu(\lambda = 308\text{ nm}) \rightarrow \text{photoproducts} \quad \text{(R1)}$$

End-photoproducts formed in the pulsed laser photolysis of CF_3CH_2CHO at 298 K were identified by Fourier transform infrared (FTIR) spectroscopy. The formation of the products is interpreted based on a proposed mechanism. Additionally, the UV absorption cross sections (σ_λ) for CF_3CH_2CHO between 230 and 350 nm as a function of temperature (269–323 K) were measured by gas-phase UV spectroscopy. Based on these results, the photolysis rates for CF_3CH_2CHO were calculated using a radiation transfer model. These results are discussed in terms of the role of CF_3CH_2CHO photolysis with respect to removal initiated by OH radicals in the troposphere.

Experimental details

Gas-phase UV absorption spectroscopy

The absorption spectra of CF_3CH_2CHO were measured between 230 and 350 nm using a single beam apparatus consisting of a 0.5 m spectrograph equipped with a 300 grooves per mm grating.[11–13] The resolution of the spectrograph was 0.18 nm. Wavelengths were calibrated using a pen-ray Hg lamp. The wavelength calibration reproduces the position of the Hg lines within an uncertainty of less than 0.06%. The radiation source was an Oriel deuterium lamp and the detector was a coupled-charge device cooled by a Peltier system. The Pyrex absorption cell (path length, ℓ = 107 cm) was surrounded by an outer jacket. The temperature (269–323 K) regulation was provided by a fluid circulating by means of a thermostatic bath (Huber, Polystat CC1) through the outer jacket (distilled water was used at $T \geq 298$ K and ethanol at $T < 298$ K). Pressure inside the absorption cell ranged from 1.0 to 7.4 Torr and was measured by a capacitance pressure transducer. Absorption spectra of the evacuated cell and of the cell filled with a gas sample were alternately recorded several times. The absorption cross sections at the wavelength λ (in base e) and temperature T, σ_λ, were obtained from the slope of the Beer–Lambert plots as previously described:[11–13]

$$A_\lambda = \ln\frac{I_{0,\lambda}}{I_\lambda} = \sigma_\lambda \ell c \quad \text{(E2)}$$

These plots were linear in the pressure range studied, as shown in Fig. S1 of the ESI.† This procedure was repeated at least three times at each temperature. An average absorption cross section is then derived.

Pulsed laser photolysis at 308 nm of CF_3CH_2CHO/air mixtures

The experimental set-up is depicted in Fig. S2 of the ESI.† It consists in a photolysis gas cell (ℓ = 10 cm and $\varnothing$ = 2 cm) sealed with quartz windows. The cell was filled with a total pressure between 25.4 and 760 Torr of a mixture containing CF_3CH_2CHO (dilution factor ranged from 2.03×10^{-3} to 2.76×10^{-3}) and synthetic air. Several pressure transducers were used to measure the pressure during the preparation of the bulb (Leybold CERAVAC CTR90, range 10 Torr and Inficon SKY CR090, range 1000 Torr) and the pressure inside the photolysis cell (Leybold CERAVAC CTR90, range 100 Torr and Edwards Barocel 600AB, range 1000 Torr). O_2 present in the air mixture scavenges alkyl (R) or acyl (RCO) radicals formed in reaction (R1). Cyclohexane (35.1–40.2 Torr diluted in 705–870 Torr of air) was also added to the gas mixture as an OH radical scavenger (see the Results and discussion section).

Prior to performing the photolysis experiments, a diluted mixture of CF_3CH_2CHO was kept in the cell in the dark for the same timescale as the experiments performed here. No aldehyde loss was observed during these test experiments. Before the UV irradiation of the sample, FTIR spectra between 500 and 4000 cm^{-1} were recorded with an instrumental resolution of 1 cm^{-1}. The FTIR spectrometer employed (Bruker, Tensor 27) has been recently described by Antiñolo *et al.*[8] The static sample was then irradiated with a pulsed XeCl excimer laser (Lambda Physik, LPX100). Irradiation times ranged from 5 to 20 min, *i.e.*, 3000 to 12 000 laser pulses at 308 nm at a repetition rate of 10 Hz. The laser beam was expanded by means of a cylindrical plane-convex lens (Melles Griot, −40 mm focal length) to irradiate the entire gas volume. The measured energy per pulse ranged from 14.7 to 32.0 mJ $pulse^{-1}$ and was monitored by a NIST calibrated calorimetric disc (OPHIR, PE50-SH-V2) at the exit of the photolysis cell. Absorption by the windows at 308 nm was taken into account to correct the laser fluence (10.5–16.0 mJ cm^{-2} $pulse^{-1}$). The laser fluence was verified by using NO_2 and CH_3CHO as chemical actinometers. Since NO_2 photolyses to a greater extent than CF_3CH_2CHO and CH_3CHO, only a few laser shots (100–200) were necessary to deplete from 8 to 18% of the NO_2. The laser fluence obtained using NO_2 and CH_3CHO actinometers is in fair agreement (within ±20%, at a 95% confidence level) with those from the calorimetric disk. Therefore, this uncertainty has been quadratically added to the statistical uncertainty in the reported photolysis quantum yields.

After irradiation with n laser pulses (n = 3000–12 000), the sample of diluted CF_3CH_2CHO was expanded into the FTIR gas cell (1.33 L) and a mercury cadmium telluride (MCT) detector was used to analyze the contents of the photolysis cell over the spectral region between 500 and 4000 cm^{-1}. The 1732–1774 cm^{-1} band for CF_3CH_2CHO was used to monitor the temporal profile of the fluorinated aldehyde. After subtracting the carbonyl photolysis products which interfere in the analysis (see Results and discussion section), the single exponential decay of this band (A) followed the integrated rate equation:

$$\ln\frac{A_0}{A_n} = \frac{J_{308\text{nm}}(\text{s}^{-1})}{10(\text{pulse s}^{-1})} n(\text{pulses}) \quad \text{(E3)}$$

where A_n and A_0 are the integrated absorbances (A_{int}) between $\tilde{\nu}_1$ and $\tilde{\nu}_2$ after n pulses and before irradiating each renewed sample, respectively. A_{int} is given by the equation:

$$A_{int} = \int_{\tilde{\nu}_1}^{\tilde{\nu}_2} A(\tilde{\nu})d\tilde{\nu} \qquad \text{(E4)}$$

The photolysis rate coefficient at 308 nm employed (J_{308nm}) for CF_3CH_2CHO was then obtained from the slope of the plots of $\ln(A_0/A_n)$ *versus* n. Since the photolysis rate at a wavelength λ, J_λ, is given by:

$$J_\lambda = \Phi_\lambda \sigma_\lambda E_\lambda, \qquad \text{(E5)}$$

the photolysis quantum yield Φ_λ can be then obtained, using the irradiance of the laser (E_λ in photon cm^{-2} s^{-1}) and the absorption cross section at this wavelength. This procedure was repeated for each total pressure. The fraction of CF_3CH_2CHO photolyzed per pulse, *i.e.* $\sigma_\lambda \Phi_\lambda E_\lambda$, is *ca.* 10^{-5} molecule per pulse, thus eqn (E3) can be used to derive Φ_λ.

Reagents. Liquid samples were used after degasification at 77 K (purities are given in brackets): CF_3CH_2CHO (97%) from Apollo Scientific Ltd, cyclohexane (>99.9%), CH_3CHO (99.5%), $CF_3CH_2C(O)OH$ (98%), and CF_3CH_2OH (>99%) from Aldrich and HC(O)OH (98–100%) from Riedel-de Häen. Gases from Praxair were used as supplied: synthetic air (99.999%), NO_2 (98%), and CO (99.998%).

Results and discussion

UV absorption cross sections (σ_λ) as a function of temperature

In Table S1 of the ESI†, averaged σ_λ for CF_3CH_2CHO between 230 and 350 nm are listed at each nm as a function of temperature (269–323 K). These absorption spectra, presented in Fig. 1a, exhibit a weak structured band as a result of the symmetry-forbidden n → π* transition in the carbonyl group. At all temperatures the position of the absorption maximum of this band, λ_{max}, appears at (290.82 ± 0.22) nm (±2σ, twice the standard deviation of the mean). The averaged maximum absorption cross section at room temperature, $\sigma_{\lambda_{max}}$ = (3.59 ± 0.24) × 10^{-20} cm^2 $molecule^{-1}$ (±2σ), for CF_3CH_2CHO is shown in Table 1 together with those from bibliography.[9,10] The position of the absorption peak differs in 1 nm and 2 nm from previous data reported by Sellevåg *et al.*[9] and Chiappero *et al.*,[10] respectively. A possible explanation for such a discrepancy can be the low instrumental resolution employed by those authors (2 and 1 nm, respectively). The previously reported $\sigma_{\lambda_{max}}$ for CF_3CHO are also listed in Table 1. A slight bathochromic effect (λ_{max} around 300 nm) is observed in the CF_3CHO n → π* transition band.[9,10,14] In this work, a 9% decrease in $\sigma_{\lambda_{max}}(CF_3CH_2CHO)$ was observed between 269 and 298 K. Chiappero *et al.*[10] also reported a negligible effect of temperature on $\sigma_\lambda(CF_3CH_2CHO)$ (within the experimental uncertainty) between 269 and 298 K. A comparison between the UV absorption spectra of CF_3CH_2CHO obtained in this work at 298 K with those reported by Sellevåg *et al.*[9] and Chiappero *et al.*[10] is presented in Fig. 1b.

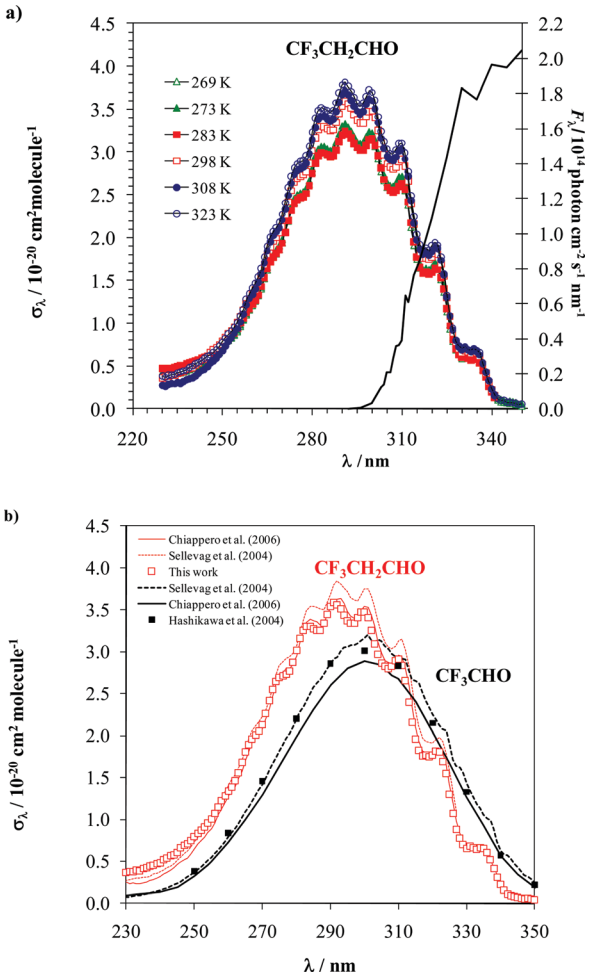

Fig. 1 (a) Absolute UV absorption spectra of CF_3CH_2CHO recorded at temperatures between 269 and 323 K. The solar spectral irradiance (F_λ) in the actinic region at 630 m of altitude is shown as a black line. (b) Comparison between UV absorption spectra of CF_3CHO and CF_3CH_2CHO at 298 K.

Table 1 Maximum absorption cross sections for CF_3CHO and CF_3CH_2CHO at 298 K

Fluoroaldehyde	λ_{max}/nm	$\sigma_{\lambda_{max}}/10^{-20}$ cm^2	Reference
CF_3CHO	300	2.89	Chiappero *et al.*[10]
	301	3.20	Sellevåg *et al.*[9]
	300	3.01	Hashikawa *et al.*[14]
CF_3CH_2CHO	290.82 ± 0.22	3.59 ± 0.24	This work[a]
	293	3.64	Chiappero *et al.*[10]
	292	3.85	Sellevåg *et al.*[9]

[a] High resolution measurements.

Photolysis quantum yield of CF_3CH_2CHO at 308 nm, $\Phi_{\lambda=308nm}$

After photolyzing a fresh sample of the same mixture during different n laser pulses, the following end-products were identified in the IR spectra: carbon monoxide (CO, 2035–2240 cm^{-1}), carbonyl fluoride (F_2CO, 1850–2000 cm^{-1}), formic acid (HC(O)OH peaks at 1775 and 1105 cm^{-1}), and trifluoroacetaldehyde (CF_3CHO, a shoulder around 1785 cm^{-1}). All these products were detected both in the absence and in the presence of the OH scavenger. Integrated areas in the 1732–1774 cm^{-1}

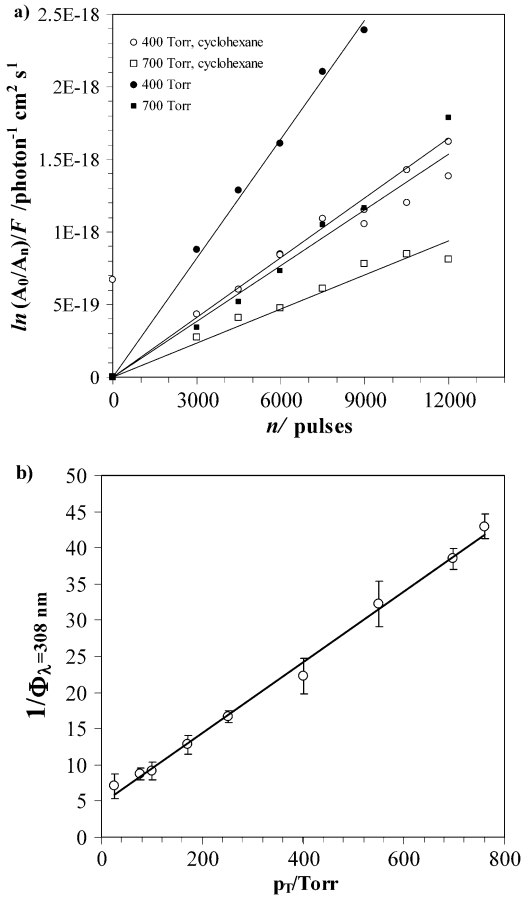

Fig. 2 (a) Decay of CF_3CH_2CHO concentration during the photolysis process at 308 nm in the absence and in the presence of cyclohexane at 400 and 700 Torr of synthetic air. (b) Stern–Volmer plot for the photolysis quantum yield at 308 nm.

region for CF_3CH_2CHO, A_n, were measured after the spectral subtraction of the features corresponding to the interfering products (HC(O)OH and CF_3CHO). An example of the decay of CF_3CH_2CHO, corrected for the measured fluence, recorded at 400 and 700 Torr is shown in Fig. 2a. The decay is faster in the absence of the OH-scavenger, indicating the importance of the OH + CF_3CH_2CHO reaction in the depletion of the fluorinated aldehyde. After 20 min of irradiation, the depletion of CF_3CH_2CHO is 56% in the absence of OH-scavenger and 26% in the presence of sufficient C_6H_{12} to remove more than 95% of the OH radicals at 400 Torr.

The photolysis quantum yields listed in Table 2 as a function of total pressure were obtained from the slope of the plots of eqn (E3) from the experiments done with added cyclohexane. Clearly, $\Phi_{\lambda=308\text{nm}}$ for CF_3CH_2CHO decreases from (0.142 ± 0.098) at 25.4 Torr to (0.023 ± 0.006) at 760 Torr. The observed effect of total pressure in Φ_λ can be parameterized by the following Stern–Volmer equation (see Fig. 2b):

$$\frac{1}{\Phi_{\lambda=308\text{nm}}} = \frac{1}{\Phi^0_{\lambda=308\text{nm}}} + \frac{K_{SV}}{\Phi^0_{\lambda=308\text{nm}}}[\text{M}] \qquad \text{(E6)}$$

The obtained quantum yield at zero pressure, $\Phi^0_{\lambda=308\text{nm}}$, is 0.22 ± 0.03 and the Stern–Volmer constant, K_{SV} is (3.25 ± 0.48) × 10^{-19} cm^3 $molecule^{-1}$. The stated uncertainties are the standard deviations from the fit. K_{SV} is the ratio between the overall quenching rate coefficient, k_Q, and the dissociation rate coefficient, k_d, of excited CF_3CH_2CHO. Since the gas mixtures approximately contain 75% of N_2, 20% of O_2, 4.75% of cyclohexane and 0.25% of CF_3CH_2CHO at all total pressures, k_Q can be expressed as:

$$k_Q = 0.2k_{Q,O_2} + 0.75k_{Q,N_2} + 0.0475k_{Q,CHex} + 0.0025k_{SQ} \qquad \text{(E7)}$$

Under our experimental conditions, the self-quenching of the excited CH_3CH_2CHO is negligible, even if an upper limit of 10^{-10} cm^3 $molecule^{-1}$ s^{-1} is considered for k_{SQ}. Assuming that the excited CF_3CH_2CHO dissociates in 1 ns and considering upper limits of 10^{-10} cm^3 $molecule^{-1}$ s^{-1} for k_{Q,O_2} and k_{Q,N_2}, the contribution of cyclohexane to the quenching of excited CH_3CH_2CHO is insignificant. Therefore, the major contribution to k_Q are the quenching rate coefficients k_{Q,O_2} and k_{Q,N_2}.

Eqn (E6) was used to interpolate $\Phi_{\lambda=308\text{nm}}$ at tropospheric altitudes from the surface (p_T = 760 Torr) to 10 km (p_T = 170 Torr). The pressure dependence of the quantum yield may then influence the estimation of the photolysis rate in the troposphere. As Table 3 shows, our determined $\Phi_{\lambda=308\text{nm}}$ is in good agreement with the effective quantum yield reported by Sellevåg *et al.*[9] at 760 Torr of air. Even though Chiappero *et al.*[10] measured $\Phi_{\lambda=308\text{nm}}$ in N_2 and in the presence of NO (700 Torr), a good accordance with our results is found within the experimental uncertainties.

At 1 bar, the photolysis quantum yield for CH_3CHO ($\Phi_{\lambda=308\text{nm}}$ = 0.32)[15] and CH_3CH_2CHO ($\Phi_{\lambda=308\text{nm}}$ = 1)[15] is much higher than that for the corresponding fluorinated aldehydes, CF_3CHO (Φ < 0.02, 292–400 nm)[10] and CF_3CH_2CHO ($\Phi_{\lambda=308\text{nm}}$ = 0.023). Hence, the exchange of the methyl group in the non-fluorinated aldehydes by a $-CF_3$ group provokes a strong reduction in Φ.

Table 2 Photolysis quantum yields (±2σ, uncertainties) for CF_3CH_2CHO in air at 308 nm

p_T/Torr	[M] × 10^{-19}/molecule cm^{-3}	$\Phi_{\lambda=308\text{nm}}$
25.4	0.082	0.142 ± 0.098
75.5	0.25	0.114 ± 0.045
99.4	0.32	0.109 ± 0.052
170.4	0.55	0.078 ± 0.032
250.7	0.81	0.060 ± 0.018
400.3	1.30	0.045 ± 0.019
550.5	1.78	0.031 ± 0.012
700.0	2.26	0.026 ± 0.007
760.0	2.46	0.023 ± 0.006

Table 3 Comparison of the photolysis quantum yields for CF_3CH_2CHO at 308 nm with literature values

p_T/Torr	$\Phi_{\lambda=308\text{nm}}$	Bath gas	Reference
760	0.023 ± 0.006	Air	This work
730–760	<0.04[a]	Air	Sellevåg *et al.*[9]
700	0.026 ± 0.007	Air	This work
700	0.04 ± 0.01[b]	N_2/NO	Chiappero *et al.*[10]

[a] Φ_{eff} at λ > 290 nm and relative to NO_2. [b] Relative to $(CF_3C(O))_2O$).

End-products of the photolysis of CF_3CH_2CHO at 308 nm

Examples of the FTIR spectra recorded before irradiation are presented in Fig. 3a and 4a. Spectral subtraction of cyclohexane

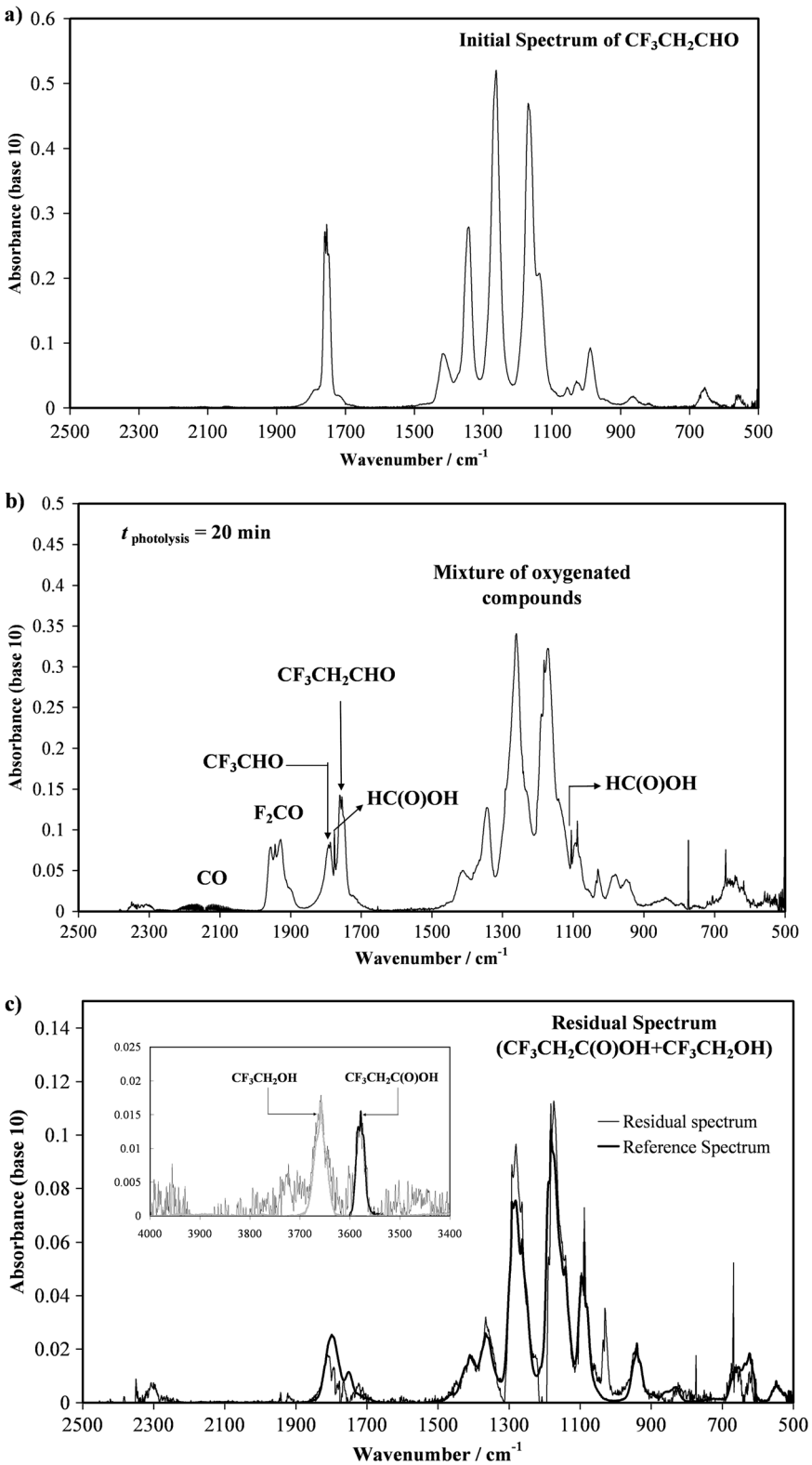

Fig. 3 FTIR spectra of CF_3CH_2CHO (3.2×10^{16} molecule cm^{-3})/air mixture in the absence of cyclohexane at 400 Torr (a) before irradiation; (b) after 12000 laser pulses (20 min) and (c) residual IR spectrum. Concentration and p_T are referred to the photolysis cell.

was performed on raw IR spectra before the analysis of the CF_3CH_2CHO band as shown in Fig. 4. Fig. 3b and 4b show the IR spectra of the sample after irradiation. As stated above, the detected products were HC(O)OH, CO, CF_3CHO, and F_2CO. To quantify HC(O)OH and CO reference spectra were recorded. The absorption cross sections reported by Sellevåg *et al.*[9] and a reference spectrum provided by Barnes[16] were used to quantify CF_3CHO and F_2CO, respectively. The infrared

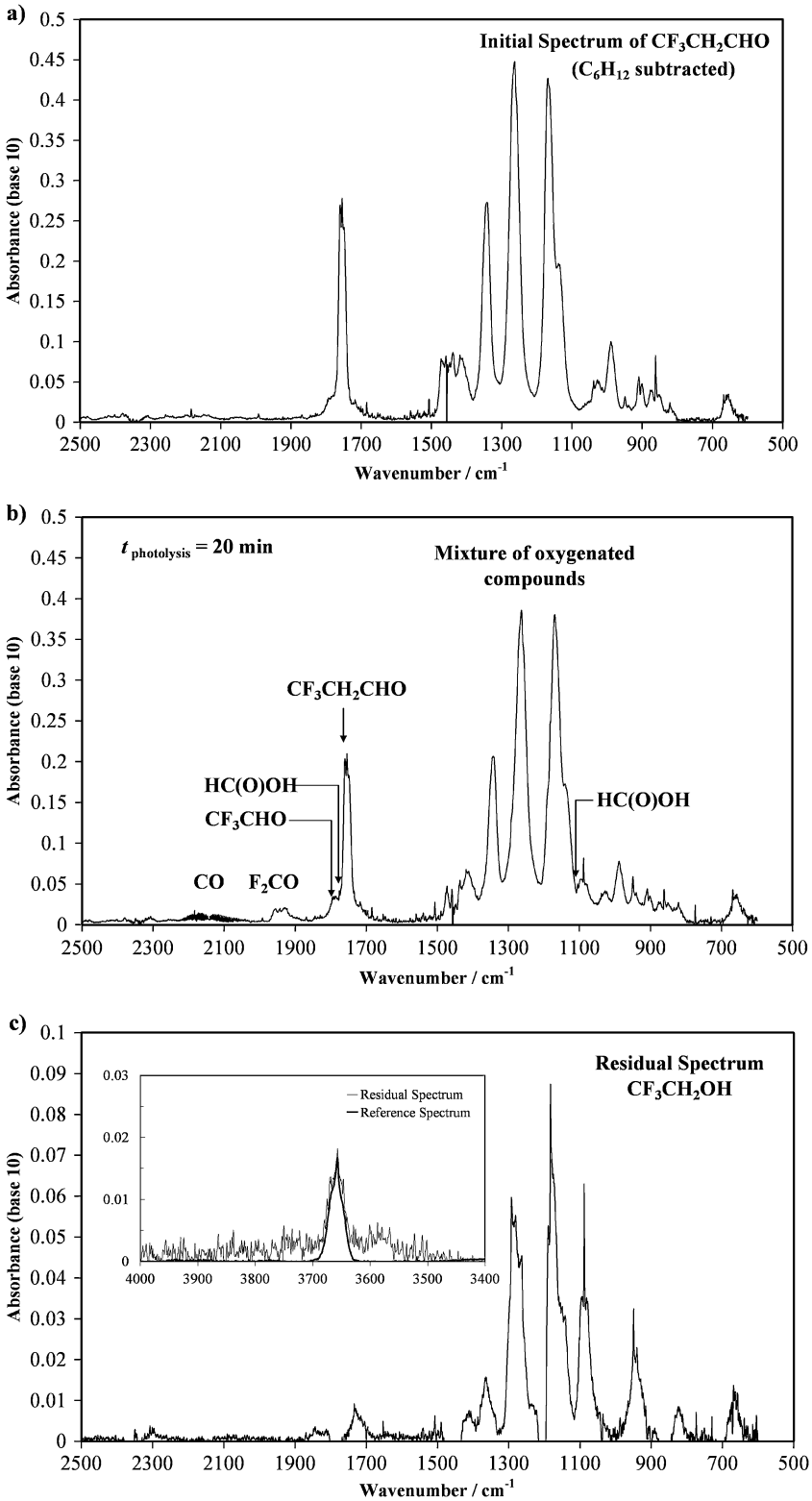

Fig. 4 FTIR spectra of CF_3CH_2CHO (3.2×10^{16} molecule cm^{-3})/air mixture in the presence of cyclohexane (1.23×10^{18} molecule cm^{-3}) at 400 Torr (a) before irradiation; (b) after 12000 laser pulses (20 min) and (c) residual IR spectrum. Concentrations and p_T are referred to the photolysis cell.

band intensities (IBI, in cm^2 $molecule^{-1}$ cm^{-1}) used in the quantification procedure are listed in Table 4. Fig. 3c and 4c show the residual spectrum after subtraction of reference spectra of CF_3CH_2CHO and all identified products mentioned above. Both in the presence and in the absence of cyclohexane, CF_3CH_2OH was observed and quantified using a reference

Table 4 Integrated infrared absorption band intensities in base 10, IBI, obtained for CF_3CH_2CHO and some detected end-products

Product	Wavenumber range/cm^{-1}	IBI/cm^2 molecule^{-1} cm^{-1}	Reference
CF_3CH_2CHO	1774–1732	5.33×10^{-18}	This work
HC(O)OH	1778–1774	1.14×10^{-18}	This work
CO	2238–2035	6.25×10^{-19}	This work
CF_3CH_2OH	3688–3629	2.81×10^{-18}	This work
CF_3CHO	1807–1779	1.08×10^{-18}	Sellevåg *et al.*[9]
F_2CO	1997–1850	2.93×10^{-17}	Barnes[16]

spectrum shown in Fig. S3a of the ESI.† In the absence of C_6H_{12} (Fig. 3c), the band centered around 3580 cm^{-1} is assigned to the O–H stretching mode of 3,3,3-trifluoropropanoic acid, $CF_3CH_2C(O)OH$. This band was not observed in the presence of the OH-scavenger, indicating that, if formed, $CF_3CH_2C(O)OH$ features lie below the detection limit (6×10^{12} molecule cm^{-3}). A reference spectrum of $CF_3CH_2C(O)OH$ is depicted in Fig. S3b (ESI†).

In the presence of cyclohexane, the concentration ranges of the end-products between 5 and 20 min were: CO ($(0.7–2.1) \times 10^{16}$ cm^{-3}), HC(O)OH ($(0.2–11.1) \times 10^{14}$ cm^{-3}), F_2CO ($(0.7–10.5) \times 10^{14}$ cm^{-3}), CF_3CHO ($(0.3–11.1) \times 10^{14}$ cm^{-3}), and CF_3CH_2OH ($(0.8–32.9) \times 10^{14}$ molecule cm^{-3}).

A proposed mechanism that could explain the formation of the observed products is presented in Table S2 (ESI†). Dissociation of CF_3CH_2CHO can occur with fission of the C–C bond to form formyl (HCO) radicals (R1a), *via* CO elimination (R1b), or by a C–H bond cleavage (R1c):

$$CF_3CH_2CHO + h\nu(\lambda = 308\ \text{nm}) \rightarrow CF_3CH_2 + HCO \quad \text{(R1a)}$$

$$\rightarrow CF_3CH_3 + CO \quad \text{(R1b)}$$

$$\rightarrow CF_3CH_2CO + H \quad \text{(R1c)}$$

A simplified mechanism for the secondary chemistry involving the radicals formed in channels (R1a) and (R1c) is shown in Scheme 1.

CO formation. Similar to Chiappero *et al.*[10] no evidence of CF_3CH_3 was observed, indicating that the Norrish type II channel (R1b) is negligible at 308 nm. Taking into account the detection limit for CF_3CH_3 in our experimental setup (S_{int}(1442–1438 cm^{-1}) = 1.08×10^{-18} cm molecule^{-1}, *ca.* 2×10^{12} molecule cm^{-3}), a relative upper limit of 5% of $\Phi_{\lambda=308\text{nm}}$ was derived for ϕ_{1b}. A higher quantum yield ϕ_{1b} would produce measurable concentrations of CF_3CH_3. Consequently, CO is mainly formed by the fast conversion of HCO radicals produced in the reaction (R1a) in the presence of O_2:

$$HCO + O_2 \rightarrow HO_2 + CO \quad \text{(R2a)}$$

An additional source of CO could be the thermal decomposition of CF_3CH_2CO radicals formed in channel (R1c), analogous to CH_3CO and CF_3CO radicals:[17–20]

$$CF_3CH_2CO \rightarrow CF_3CH_2 + CO \quad \text{(R3)}$$

Somnitz *et al.*[17] calculated the energy available for the decomposition of CH_3CO radicals formed in the photolysis of acetone at 248 nm of 134.5 kJ mol^{-1}. The internal excitation of CH_3CO, $E_{int}(CH_3CO)$, was calculated by the following equation:

$$E_{ph} + E_{int}(CH_3COCH_3) - D_0(CH_3\text{–}COCH_3) = E_{int}(CH_3) + E_{int}(CH_3CO) + E_{rel,trans} \quad \text{(E8)}$$

where E_{ph} is the photolysis energy, $E_{int}(CH_3COCH_3)$ and $D_0(CH_3\text{–}COCH_3)$ are the internal and dissociation energies of acetone, respectively, and $E_{rel,trans}$ is the relative translation energy of both photofragments. At 308 nm (E_{ph} = 388.72 kJ mol^{-1}), the maximum E_{int} of CH_3CO radicals, neglecting $E_{int}(CH_3)$ and $E_{rel,trans}$, is calculated to be *ca.* 41 kJ mol^{-1}. Additionally, Somnitz *et al.*[18] did quantum chemical calculations on CH_3CO formed in the photolysis of acetone at 248 nm and reported

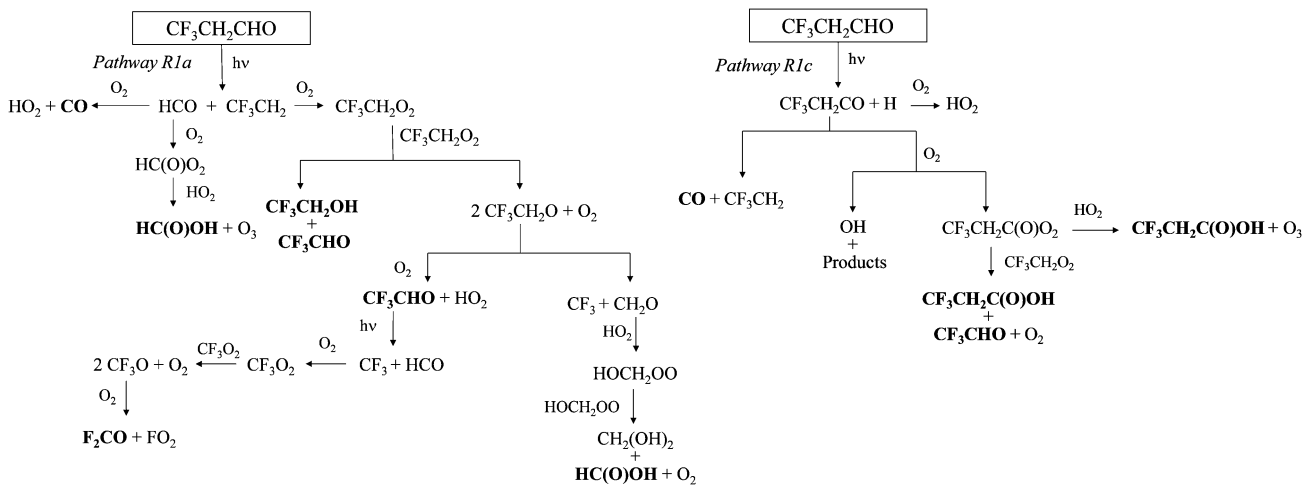

Scheme 1 A simplified reaction mechanism of the secondary chemistry due to the radicals formed in the UV photolysis of CF_3CH_2CHO. Products detected are in bold font.

that the amount of excess of energy in the vibrationally hot CH_3CO was *ca.* 65 kJ mol^{-1}. On the other hand, Tomas *et al.*[19] reported that the thermal decomposition of CF_3CO (7×10^4 s^{-1}) appeared to be much easier than that of CH_3CO (3 s^{-1}) at atmospheric pressure and that the barrier for the dissociation of CF_3CO was 49 kJ mol^{-1}.

In our case, the maximum energy available for the decomposition of CF_3CH_2CO radicals formed in reaction (R1c) can also be estimated from eqn (E8). $E_{int}(CF_3CH_2CHO)$ was calculated from the vibrational frequencies recently published by Ci *et al.*[21] $D_0(CF_3CH_2CO–H)$ was calculated from thermochemical data.[22] As a consequence, $E_{int}(CF_3CH_2CHO)$ is *ca.* 33 kJ mol^{-1}, which is similar to that available in CH_3CO and CF_3CO. Therefore, as no information on the thermal decomposition rate of CF_3CH_2CO radicals was found in the literature, we assumed the same rate coefficient for the decomposition of CF_3CO radicals.[20]

HC(O)OH formation. To our knowledge, the formation of HC(O)OH from the photooxidation of H_2CO has been reported at 295 K and 373 K.[23,24] For example, Osif and Heicklen[23] detected HC(O)OH in the Cl + H_2CO reaction in the presence of O_2 at total pressures between 62 and 704 Torr. These authors attributed the observation of HC(O)OH to a secondary chemistry of $HC(O)O_2$ radicals. Theoretical investigations on the HCO + O_2 reaction reported that it can proceed by direct H-abstraction or even exclusively *via* the formation of a $HC(O)O_2$ complex.[25,26] Energized $HC(O)O_2$ complex can be thermalised or decompose to produce CO and HO_2. In our chemical system and by analogy to the reported in the literature for $CH_3C(O)O_2$ radicals,[27] the thermalized collisional complex $HC(O)O_2$ radicals could react with HO_2 radicals, produced in reaction (R2a) and the H + O_2 reaction (R4), to form HC(O)OH (see Table S2 of the ESI†):

$$HC(O)O_2 + HO_2 \rightarrow HC(O)OH + O_3 \qquad (R5a)$$

Formation of CF_3CHO and CF_3CH_2OH. These species are likely to be formed from CF_3CH_2 radicals from reaction (R1a) and/or (R3) by the following reaction sequence:

$$CF_3CH_2 + O_2 + M \rightarrow CF_3CH_2O_2 + M \qquad (R6a)$$

$$2CF_3CH_2O_2 \rightarrow 2CF_3CH_2O + O_2 \qquad (R7a)$$

$$\rightarrow CF_3CHO + CF_3CH_2OH + O_2 \qquad (R7b)$$

$$CF_3CH_2O + O_2 \rightarrow CF_3CHO + HO_2 \qquad (R8)$$

F_2CO formation. CF_3CHO formed in reactions (R7b) and (R8) would also be photolyzed,[10]

$$CF_3CHO + h\nu(\lambda = 308\ \text{nm}) \rightarrow CF_3 + HCO, \qquad (R9)$$

producing trifluoromethyl (CF_3) radicals. These radicals can produce F_2CO in the presence of O_2 by the following reaction sequence:

$$CF_3 + O_2 + M \rightarrow CF_3O_2 + M \qquad (R10)$$

$$2CF_3O_2 \rightarrow 2CF_3O + O_2 \qquad (R11)$$

$$CF_3O + O_2 \rightarrow F_2CO + FO_2 \qquad (R12)$$

An additional source of CF_3 radicals and, hence, of F_2CO can be the thermal decomposition of CF_3CH_2O radicals formed in reaction (R7a):

$$CF_3CH_2O \rightarrow CF_3 + CH_2O \qquad (R13)$$

$CF_3CH_2C(O)OH$ formation. 3,3,3-Trifluoropropanoic acid can be formed by the oxidation of CF_3CH_2CO radicals through the following reaction sequence:

$$CF_3CH_2CO + O_2 + M \rightarrow CF_3CH_2C(O)O_2 + M \qquad (R14a)$$

$$CF_3CH_2C(O)O_2 + HO_2 \rightarrow CF_3CH_2C(O)OH + O_3 \qquad (R15a)$$

$CF_3CH_2C(O)O_2$ radicals formed in reaction (R14a), similarly to $CH_3C(O)O_2$ radicals,[28] can contribute in a lesser extent to the formation of $CF_3CH_2C(O)OH$:

$$CF_3CH_2C(O)O_2 + CF_3CH_2O_2 \rightarrow CF_3CH_2C(O)OH + CF_3CHO + O_2 \qquad (R16a)$$

As stated above, $CF_3CH_2C(O)OH$ was only detected in the photolysis experiments performed in the absence of OH-scavenger. This observation clearly indicates that channel (R1c) is not important and the main source of CF_3CH_2CO radicals seems to be the reaction of the fluorinated aldehyde with OH radicals:

$$OH + CF_3CH_2CHO \rightarrow CF_3CH_2CO + H_2O \qquad (R17)$$

The above statement is confirmed by a numerical simulation performed according to the proposed mechanism in Table S2 of the ESI.† An upper limit for ϕ_{1c} cannot be given, since most of the rate coefficients of the reactions involved in the $CF_3CH_2C(O)OH$ formation are not known.

Sources of OH radicals. Possible sources of OH radicals could be the following reactions:

$$HC(O)O_2 + HO_2 \rightarrow HC(O)O + OH + O_2 \qquad (R5c)$$

$$CF_3CH_2C(O)O_2 + HO_2 \rightarrow CF_3CH_2C(O)O + OH + O_2 \qquad (R15c)$$

Additionally, similar to other acyl radicals such as CH_3CO and C_2H_5CO,[29–31] the reaction of CF_3CH_2CO radicals with O_2 can form OH radicals in the system, particularly at low total pressures:

$$CF_3CH_2CO + O_2 \rightarrow OH + \text{products} \qquad (R14b)$$

At a constant pressure, the OH yield in the reaction of C_2H_5CO with O_2 is smaller than in the corresponding reaction with CH_3CO. The OH yield from reaction (R14b) is expected to be smaller than that for C_2H_5CO, since larger molecules normally get quenched easier. Nevertheless, the marked effect of OH-chemistry observed on the product yields indicates that the OH concentration must be sufficient to play a significant role. Under the same experimental conditions (E_λ, n, p_T, and $[CF_3CH_2CHO]_0$), the concentrations of CF_3CHO and F_2CO (Fig. 3b) and $CF_3CH_2C(O)OH$ (Fig. 3c) are larger in the absence of an OH-scavenger than in the presence of cyclohexane (Fig. 4b).

In contrast, the HC(O)OH concentration increases in the presence of an OH-scavenger. However, CO and CF_3CH_2OH concentrations remain unaltered by the presence of cyclohexane. Hence, CO seems to come almost exclusively from the conversion of HCO radicals in the presence of O_2 and the decomposition of acyl radicals.

A feasible explanation for the observed increase of the concentration of CF_3CHO and F_2CO in the absence of the OH scavenger can be related with an increase in the concentration of acyl (RCO) radicals formed in reactions (R17) and (R18):

$$OH + CF_3CHO \rightarrow CF_3CO + H_2O \qquad (R18)$$

Decomposition of CF_3CO and CF_3CH_2CO radicals would increase the concentration of CF_3 and CF_3CH_2 radicals, which are the precursors of F_2CO and CF_3CHO, respectively. Another source of F_2CO could be the following reaction:

$$OH + CF_3 \rightarrow F_2CO + HF \qquad (R19)$$

The observed $CF_3CH_2C(O)OH$ in the absence of OH-scavenger could result from the increase of $CF_3CH_2C(O)O_2$ radicals, coming from CF_3CH_2CO radicals formed in (R17). On the other hand, the observed increase in the HC(O)OH concentration in the presence of cyclohexane could be related to the larger contribution of the HO_2-reactions (R5a). In addition, the $HO_2 + CH_2O$ reaction could be a source of hydroxymethylperoxyl radicals ($HOCH_2OO$) which further react to form HC(O)OH:[28]

$$HO_2 + CH_2O \rightarrow HOCH_2OO \qquad (R20)$$

$$2HOCH_2OO \rightarrow HC(O)OH + CH_2(OH)_2 + O_2 \qquad (R21a)$$

$$\rightarrow 2HOCH_2O + O_2 \qquad (R21b)$$

However, HC(O)OH concentrations simulated according to the reaction sequence (R20)–(R21) were several orders of magnitude lower than those measured here.

Temporal evolution of end-products. An example of the experimental temporal profiles of several end-products is shown in Fig. 5 for an experiment performed in the presence of an OH-scavenger at 400 Torr (open circles). Fig. 5 also displays the results from the numerical simulation employing the reaction mechanism proposed in Table S2 of the ESI.†

Although the branching ratio $\alpha = \phi_{1a}/\phi_{1c}$ cannot be directly determined in this work due to the uncertainties in the rate coefficients (R5a)–(R5c) which were taken as those from the $CH_3C(O)O_2 + HO_2$ reaction (for (R5b) see Table S2 of the ESI†),[15,28] the time evolution of HC(O)OH could provide insight into the relative importance of photolysis channels (R1a) and (R1c). Accordingly, the branching ratio between the rate coefficients for the direct H-abstraction of HCO by O_2 (R2a) and the $HC(O)O_2$ complex formation (R2b) (see Table S2 of the ESI†), β, will directly affect the calculated temporal profiles of HC(O)OH and, therefore, the value of α. To our knowledge, experimental data on the determination of β are scarce. Osif and Heicklen[23] reported a branching ratio

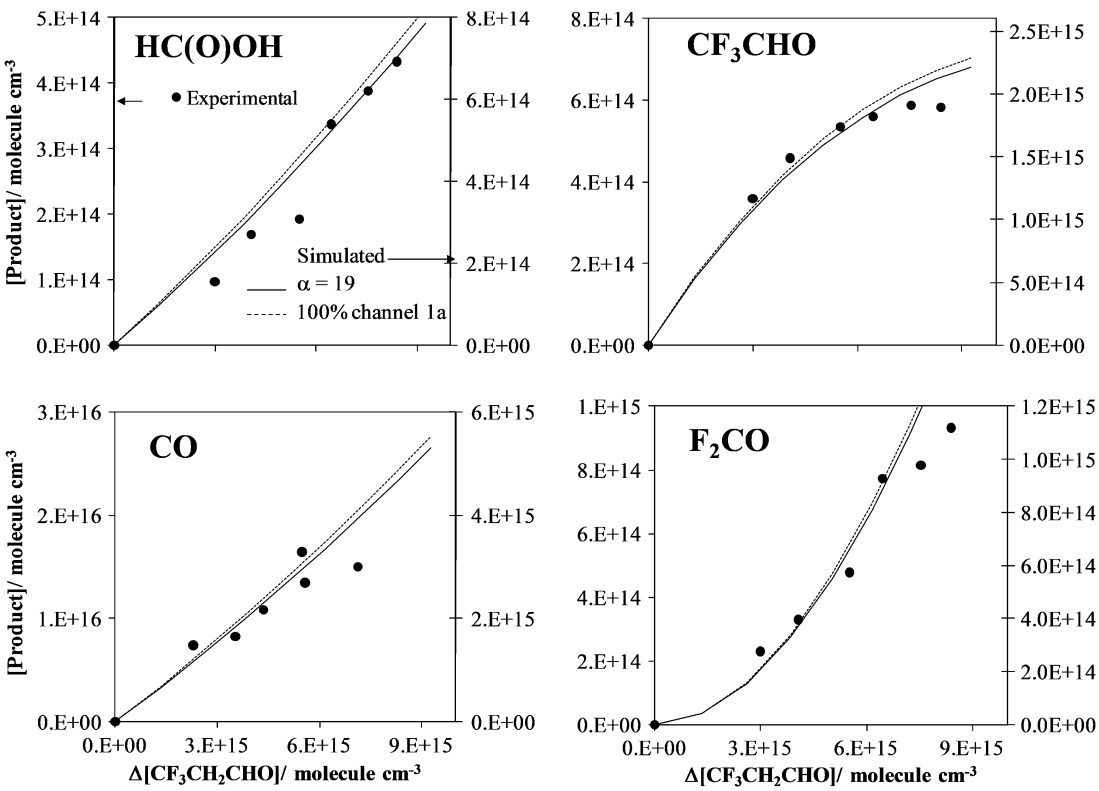

Fig. 5 Experimental (symbols and the left-hand side y-axis) and predicted (line and the right-hand side y-axis) evolution of the detected products in the photolysis of CF_3CH_2CHO at 308 nm as a function of the aldehyde loss at 400 Torr of air. The lines are the simulated profile according to the mechanism proposed in Table S2 (ESI†). A $\beta = k_{2a}/k_{2b}$ of unity was used in the simulation to derive the branching ratio $\alpha = \phi_{1a}/\phi_{1c}$.

β = 0.2 between 60 and 700 Torr of air, which contradicts with the previous work of Demerjian *et al.*[32] who reported a value of β = 0.04. Recent quantum RRK calculations from Bozzelli and Dean[25] show that β increases from roughly 0.45 at 760 Torr to 8 at 76 Torr at 300 K. These calculations are consistent with the observed increase of [HC(O)OH] with total pressure for a constant $\Delta[CF_3CH_2CHO]$. An attempt to derive α was made by using the theoretical β of 1 at 400 Torr and the well-known overall rate coefficient, $k_2 = 5.2 \times 10^{-12}$ cm^3 molecule^{-1} s^{-1}. Bozzelli and Dean[25] proposed that $HC(O)O_2$ radical formed in (R2b) isomerizes to (O)COOH (2.6×10^{-13} cm^3 molecule^{-1} s^{-1}), which rapidly decomposes (7.4×10^4 s^{-1}) to yield HO_2 and CO. In this case, the temporal profile of HC(O)OH is well reproduced adjusting α to 19 (95% of CF_3CH_2CHO would undergo photolysis *via* C–C bond cleavage) or even if HCO and CF_3CH_2 radicals are considered the only photoproducts in the photolysis of CF_3CH_2CHO. This is consistent with our experimental observations. However, further studies are needed to clarify the formation of HC(O)OH from HCO radicals.

For F_2CO and CF_3CHO the simulated concentration profiles are neither directly comparable to the experimentally observed profiles due to a number of assumptions used in the calculation. Specific assumptions are: (i) rate coefficients for the reactions involving fluorinated radicals (except for CF_3, CF_3O, and CF_3O_2) are unknown and assumed to be equal to those of the corresponding fully hydrogenated radicals; and (ii) the photolysis rate of CF_3CHO was calculated using the photolysis quantum yield reported by Chiappero *et al.* at 700 Torr.[10] However, it is likely that the quantum yield is larger at 400 Torr.

Despite the significant uncertainties in the proposed mechanism, the experimental and simulated profiles present similar trends. Hence, additional kinetic and mechanistic studies of the reactions of fluorinated radicals could further elucidate the reaction mechanism responsible for the product formation.

Photolysis rate coefficients (*J*) in the troposphere

Since gas density in the atmosphere decreases with altitude, the wavelength and pressure dependence of σ_λ and Φ_λ is important for estimating the atmospheric photolysis rate of CF_3CH_2CHO. In addition, the calculation of F_λ at a specific zenith angle or location is needed to estimate the photolysis rate throughout the troposphere. As the available F_λ data are tabulated in a wavelength interval, $\Delta\lambda$, eqn (E1) can be rewritten as follows:

$$J \cong \Sigma\sigma_\lambda\Phi_\lambda F_\lambda\Delta\lambda \qquad \text{(E9)}$$

F_λ calculations were carried out by using the TUV radiative transfer model (4.1 version) developed by Madronich and Flocke.[33] A 4-stream discrete ordinate method was used for all the radiative transfer calculations, with cloudless and aerosol-free sky conditions. Latitude and longitude were set for Ciudad Real, Spain. In all the calculations, the overhead ozone column was set as 300 Dobson units. The pressure dependence of $\Phi_{\lambda=308\text{nm}}$ and σ_λ reported here were used in the J calculation. The wavelength dependence of Φ_λ is not known at all total pressures. Only at 700 Torr, the photolysis quantum yield of CF_3CH_2CHO seems to be strongly dependent on wavelength ($\Phi_{\lambda=254\text{nm}}$ = (0.74 ± 0.08)[10] and $\Phi_{\lambda=308\text{nm}}$ = (0.026 ± 0.007) from this work). No information on the pressure dependence of the photolysis quantum yield of CF_3CH_2CHO was found at other wavelengths. Nevertheless, it is expected that the pressure dependence of Φ_λ be stronger at longer wavelengths than 308 nm and be much weaker at wavelengths between 290 and 308 nm. So, further studies are needed to have a complete understanding of the Φ_λ as a function of total pressure.

The lifetime of CF_3CH_2CHO due to the OH-reaction has been recently estimated to be from 4 days at the surface to 6 days in the upper troposphere.[8] As CF_3CH_2CHO is a very short-lived species, compared with the tropospheric vertical mixing time (1–2 months), it is not expected to reach the upper troposphere (10–12 km), unless this aldehyde is formed in this region by OH-reactions with fluorinated compounds with longer lifetimes. Even though CF_3CH_2CHO is not uniformly distributed, it is worthwhile to quantify J as a function of altitude to have a complete vision of its influence. In the estimation of J, $\Phi_{\lambda=308\text{nm}}$ and its pressure dependence are assumed to be constant in the actinic region. Therefore, upper limits of the photolysis rates are reported here, 2.83×10^{-6} s^{-1} and 1.0×10^{-5} s^{-1} at the ground level and 10 km, respectively. Besides, even if there were a shift of 1 nm in the absorption spectrum of CF_3CH_2CHO, the estimated photolysis rate would increase *ca.* 7%. However, it is important to note that the assumption of a wavelength independent quantum yield would also produce a decrease in the overall J value. The overall lifetime of CF_3CH_2CHO in the troposphere can be defined as follows:

$$\tau = \frac{1}{J + \sum k_{\text{Oxid}}[\text{Oxid}]_{\text{avg}}} \qquad \text{(E10)}$$

where k_{Oxid} is the rate coefficient of the reaction of the aldehyde i with the oxidant (OH, NO_3, O_3, or Cl) and $[\text{Oxid}]_{\text{avg}}$ is the 24 h averaged concentration of the corresponding oxidant in the troposphere (1×10^6 radical cm^{-3} for OH).[34] Reactions with NO_3 and O_3 are expected to be a negligible sink

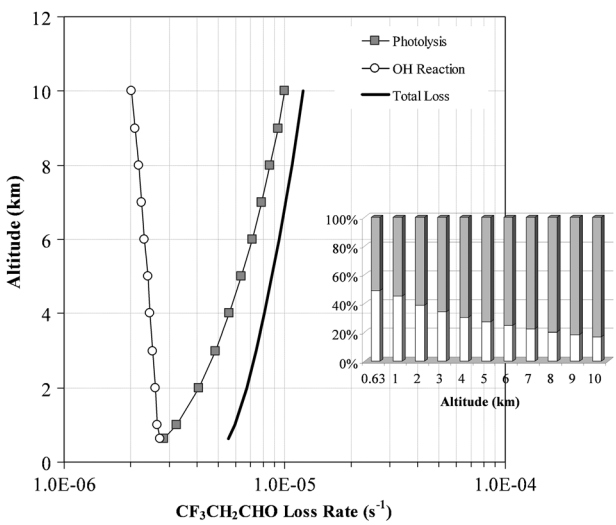

Fig. 6 First-order loss rate of CF_3CH_2CHO due to the removal by OH radicals and UV photolysis is plotted as a function of altitude. Percentage of the contribution of both removal processes at each altitude is presented at right-hand side.

of CF_3CH_2CHO compared with its removal by OH radicals. In Fig. 6, a comparison of the first-order rate for the homogeneous removal and the UV photolysis process of CF_3CH_2CHO is shown together with the overall rate loss, k_{loss} ($= J + k_{OH}[OH]_{avg}$). The overall lifetime of CF_3CH_2CHO is estimated to be $\sim$2 days at the ground level and 1 day at higher altitudes in the troposphere. The upper limit for the contribution of the photolysis of CF_3CH_2CHO to k_{loss} could range from 50% at the ground level up to 80% at 10 km. According to this study, in unpolluted atmospheres the expected products of the photodegradation of CF_3CH_2CHO can be CO, F_2CO, HC(O)OH, CF_3CHO, $CF_3CH_2C(O)OH$, and CF_3CH_2OH. However, the volume mixing ratio of CF_3CH_2CHO used in this work is several orders of magnitude higher than that expected in the atmosphere and, therefore, at the expected levels of CF_3CH_2CHO in the atmosphere, none of photodegradation products pose any environmental threat.

Conclusions

In this work, we report (i) the temperature dependence of the UV absorption cross sections of CF_3CH_2CHO between 269 and 323 K; (ii) the first study on the pressure dependence of $\Phi_{\lambda=308nm}$ in CF_3CH_2CHO/air/cyclohexane mixtures, (iii) the quantification of the final products (CO, HC(O)OH, CF_3CHO, F_2CO, and CF_3CH_2OH) by FTIR spectroscopy, and (iv) a proposed mechanism that justifies the observed final products and their temporal evolution.

Knowing the photolysis quantum yield at tropospheric pressures is of great importance in order to better determine the photolysis lifetime of this fluorinated aldehyde. On the other hand, the wavelength dependence of Φ_λ in the actinic region ($\lambda \geq 290$ nm) is also needed to better quantify any photolysis process in the troposphere. In this work, the photolysis quantum yield of CF_3CH_2CHO at 308 nm has been reported to decrease with total pressure. If a similar behaviour is considered for Φ_λ at other wavelengths, the photolysis rate J at higher altitudes in the troposphere would be more important than reported, since F_λ and Φ_λ increases with altitude.

Acknowledgements

The authors would like to thank the Spanish Ministerio de Ciencia e Innovación (MICINN) (CGL2007-61835/CLI and CGL2010-19066) and the Consejería de Educación y Ciencia de la Junta de Comunidades de Castilla-La Mancha (PEII11-0279-8538) for supporting this Project. M. Antiñolo wishes to thank MICINN for providing her a grant (AP2007-02706). We would also like to thank Prof. Ian Barnes for providing a reference spectrum of F_2CO and Dr Christa Fittschen and Dr Mary K. Gilles for helpful discussions.

References

1 J. S. Daniel and G. J. M. Velders (Lead Authors). Halocarbon Scenarios, Ozone Depletion Potentials, and Global Warming Potentials, in *Scientific Assessment of Ozone Depletion: 2006*, Global Ozone Research and Monitoring Project-Report No. 50, World Meteorological Organization, Geneva, Switzerland, 2007, ch. 8.
2 E. Jiménez, M. Antiñolo, B. Ballesteros, E. Martínez and J. Albaladejo, *ChemPhysChem*, 2010, **11**, 4079–4087.
3 T. Kelly, V. Bossoutrot, I. Magneron, K. Wirtz, J. Treacy, A. Mellouki, H. Sidebottom and G. Le Bras, *J. Phys. Chem. A*, 2005, **109**, 347–355.
4 M. D. Hurley, J. A. Misner, J. C. Ball, T. J. Wallington, D. A. Ellis, J. W. Martin, S. A. Mabury and M. P. Sulbaek Andersen, *J. Phys. Chem. A*, 2005, **109**, 9816–9826.
5 M. D. Hurley, T. J. Wallington, M. P. Sulbaek Andersen, D. A. Ellis, J. W. Martin and S. A. Mabury, *J. Phys. Chem. A*, 2004, **108**, 1973–1979.
6 L. Chen, N. Takenaka, H. Bandow and Y. Maeda, *Atmos. Environ.*, 2003, **37**, 4817–4822.
7 R. Atkinson, D. L. Baulch, R. A. Cox, J. N. Crowley, R. F. Hampson, R. G. Hynes, M. E. Jenkin, M. J. Rossi, J. Troe and T. J. Wallington, *Atmos. Chem. Phys.*, 2008, **8**, 4141–4496.
8 M. Antiñolo, E. Jiménez, A. Notario, E. Martínez and J. Albaladejo, *Atmos. Chem. Phys.*, 2010, **10**, 1911–1922.
9 S. R. Sellevåg, T. Kelly, H. Sidebottom and C. J. Nielsen, *Phys. Chem. Chem. Phys.*, 2004, **6**, 1243–1252.
10 M. S. Chiappero, F. E. Malanca, G. A. Argüello, S. T. Wooldridge, M. D. Hurley, J. C. Ball, T. J. Wallington, R. L. Waterland and R. C. Buck, *J. Phys. Chem. A*, 2006, **110**, 11944–11953.
11 E. Jiménez, B. Lanza, E. Martínez and J. Albaladejo, *Atmos. Chem. Phys.*, 2007, **7**, 1565–1574.
12 B. Lanza, E. Jiménez, B. Ballesteros and J. Albaladejo, *Chem. Phys. Lett.*, 2008, **454**, 184–189.
13 E. Jiménez, B. Lanza, M. Antiñolo and J. Albaladejo, *Environ. Sci. Technol.*, 2009, **43**, 1831–1837.
14 Y. Hashikawa, M. Kawasaki, R. L. Waterland, M. D. Hurley, J. C. Ball, T. J. Wallington, M. P. Sulbaek Andersen and O. J. Nielsen, *J. Fluorine Chem.*, 2004, **125**, 1925–1932.
15 R. Atkinson, D. L. Baulch, R. A. Cox, J. N. Crowley, R. F. Hampson, R. G. Hynes, M. E. Jenkin, M. J. Rossi and J. Troe, *Atmos. Chem. Phys.*, 2006, **6**, 3625–4055.
16 I. Barnes. Personal communication.
17 H. Somnitz, M. Fida, T. Ufer and R. Zellner, *Phys. Chem. Chem. Phys.*, 2005, **7**, 3342–3352.
18 H. Somnitz, T. Ufer and R. Zellner, *Phys. Chem. Chem. Phys.*, 2009, **11**, 8522–8531.
19 A. Tomas, F. Caralp and R. Lesclaux, *Z. Phys. Chem.*, 2000, **214**, 1349–1365.
20 M. M. Maricq, J. J. Szente, G. A. Khitrov, T. S. Dibble and J. S. Francisco, *J. Phys. Chem.*, 1995, **99**, 11875–11882.
21 C. G. Ci, H. B. Yu, S. Q. Wan, J. Y. Liu and C. C. Sun, *Bull. Korean Chem. Soc.*, 2011, **32**, 1187–1194.
22 S. P. Sander, J. Abbatt, J. R. Barker, J. B. Burkholder, R. R. Friedl, D. M. Golden, R. E. Huie, C. E. Kolb, M. J. Kurylo, G. K. Moortgat, V. L. Orkin and P. H. Wine, *Chemical Kinetics and Photochemical Data for Use in Atmospheric Studies, Evaluation No. 17*, JPL Publication 10-6, Jet Propulsion Laboratory, Pasadena, 2011.
23 T. L. Osif and J. Heicklen, *J. Phys. Chem.*, 1976, **80**, 1526–1531.
24 J. E. Carruthers and R. G. W. Norrish, *J. Chem. Soc.*, 1936, 1036–1042.
25 J. W. Bozelli and A. M. Dean, *J. Phys. Chem.*, 1993, **97**, 4427–4441.
26 M. Martínez-Ávila, J. Peiró-García, V. M. Ramírez-Ramírez and I. Nebot-Gil, *Chem. Phys. Lett.*, 2003, **370**, 313–318.
27 T. J. Dillon and J. N. Crowley, *Atmos. Chem. Phys.*, 2008, **8**, 4877–4889.
28 http://www.iupac-kinetic.ch.cam.ac.uk/.
29 M. A. Blitz, D. E. Heard and M. J. Pilling, *Chem. Phys. Lett.*, 2002, **365**, 374–379.
30 S. A. Carr, M. T. Baeza-Romero, M. A. Blitz, M. J. Pilling, D. E. Heard and P. W. Seakins, *Chem. Phys. Lett.*, 2007, **445**, 108–112.
31 M. T. Baeza Romero, M. A. Blitz, D. E. Heard, M. J. Pilling, B. Price, P. W. Seakins and L. Wang, *Faraday Discuss.*, 2005, **130**, 73–88.
32 K. L. Demerjian, J. A. Kerr and J. G. Calvert, *Adv. Environ. Sci. Technol.*, 1974, **4**, 1–262.
33 S. Madronich and S. Flocke, *The role of solar radiation in atmospheric chemistry*, in *Handbook of Environmental Chemistry*, ed. P. Boule, Springer-Verlag, Heidelberg, 1999, pp. 1–26.
34 M. Krol, P. J. van Leeuwen and J. Lelieveld, *J. Geophys. Res., [Atmos.]*, 1998, **103**, 10697–10711.

